Lehrstuhl für Bildverarbeitung
Institute of Imaging & Computer Vision

Control algorithms for large scale, single axis photovoltaic trackers

Dorian Schneider

Institute of Imaging and Computer Vision
RWTH Aachen University, 52056 Aachen, Germany
tel: +49 241 80 27860, fax: +49 241 80 22200
web: www.lfb.rwth-aachen.de

in: Proceedings of the 16th International Student Conference on Electrical Engineering POSTER 2012.
See also BibTeX entry below.

BibTeX:

```
@inproceedings{DS2012a,
author = {Dorian Schneider},
title = {Control algorithms for large scale, single axis photovoltaic trackers},
booktitle = {Proceedings of the 16th International Student Conference on Electrical Engineering POSTER 2012},
address = {Prague, Czech Republic},
month = {May 17},
year = {2012}
}
```


document created on: January 21, 2013
created from file: HER10a.tex
cover page automatically created with CoverPage.sty
(available at your favourite CTAN mirror)

RWTH AACHEN
RHEINISCH-WESTFÄLISCHE TECHNISCHE HOCHSCHULE AACHEN

Control algorithms for large scale, single axis photovoltaic trackers

Dorian Schneider

Institute of Imaging & Computer Vision, RWTH Aachen University, 52056 Aachen

schneider@lfb.rwth-aachen.de

Abstract. *The electrical yield of large scale photovoltaic power plants can be greatly optimized by employing solar trackers. While fixed-tilt superstructures are stationary and immobile, trackers move the PV-module plane in order to optimize its alignment to the sun. This paper introduces control algorithms for single-axis trackers (SAT) including a discussion for optimal alignment and backtracking. The results are used to simulate and compare the electrical yield of fixed-tilt and SAT systems. The proposed algorithms are field tested and on duty in solar parks world-wide.*

Keywords

single axis solar tracker, backtracking, photovoltaic, sun tracking

1. Introduction

The degree efficiency of photovoltaic (PV) power plants can be maximized by optimizing the alignment of the photovoltaic module plane to the current position of the sun. On the opposite to fixed-tilt superstructures where modules are placed stationary in the field, tracking superstructures mount the modules on carriers able to rotate along one or two axis in order to maximize the electrical yield of the system. Two different schemes for the construction of a PV-tracker exist: Dual-Axis Trackers (DAT) are provided with two degrees of freedom which theoretically allows an optimal module-sun alignment and hence the maximum possible yield at any time. Theoretically, DATs allow a raise of 30% - 45% [7] in yield compared to an optimal positioned fixed-tilt plant at the same location. The details for tracker performances and extra yield have high variance, since they strongly depend on the location where the system is installed [8]. The benefits of DATs are paid with augmented need for space such as higher mechanical complexity involving raised costs for construction, planing and attendance. On the other hand, Single-Axis Trackers (SAT) provide only one degree of freedom, limiting the tracking motion so that perfect module-sun alignment can not always be provided. Even though the tracking angle is limited, the system can provide incremented yields of 10%-20% compared to a perfectly adjusted fixed-tilt plant at the same location. The constructional complexity is significantly decreased compared to DATs, affecting the costs for construction and attendance in a positive way.

In order to choose the best system for a power-plant of given size and location, one needs to optimize the cost-yield ratio of the system. While the costs for construction and attendance can be estimated easily, expected yields can only be analysed using sophisticated simulations.

While several algorithms and controlling schemes for high precision DAT control have been published [1, 2, 3, 6] very few publication handle the control of SATs. In fact, the results found in [4, 5] are estimations and give not an enclosed solution for the backtracking problem. For this reason, this paper introduces control algorithms for SATs which allow to regulate the system to the optimal position at any time without the need for any additional sensor technology or hardware but using the calculated sun position instead. The problem of self-shadowing is addressed with a high precision, field-tested backtracking algorithm. The results are used for a basic energy yield analysis.

The paper structure is given as follows. In section 2, the nomenclature and coordinate system for later sections are defined. Section 3 handles the basic mathematical equations for naive tracking, allowing the system to find the rotation angle that maximizes the yield for a given sun position. Since the system should avoid self-shadowing by all means, a backtracking algorithm that finds an optimal shadow free rotation angle is discussed in section 4. The results are affiliated in section 5 to simulate SAT yield expectations for different latitudes and superstructure settings in Matlab/Simulink. Section 6 discusses the results and section 7 concludes the work.

2. Coordinate system

We define the nomenclature and coordinate system that is used throughout the subsequent sections. Due to the rotational movement of the sun, a polar coordinate system is used as illustrated in Fig. 1: Here, the azimuth angle ϕ is given by the angle between the orthogonal projection of the

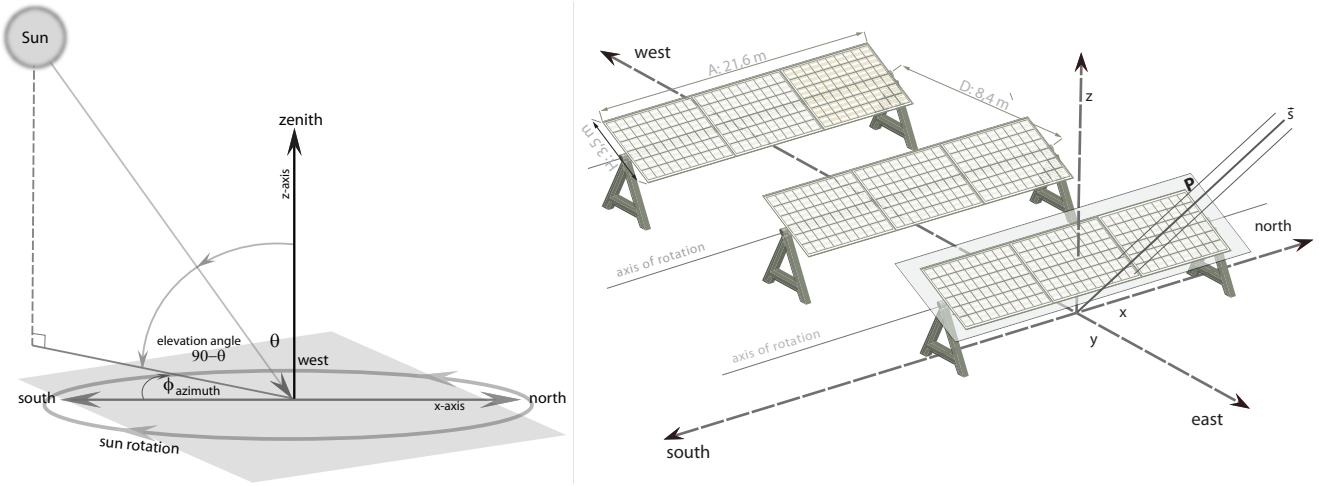

Fig. 1: Schemes of the SAT coordinate system. Left: illustration of sun azimuth and elevation angles. Right: Illustration of three adjacent SATs with corresponding distances and annotations.

sun vector **s** to the xy-plane and the x-axis (north-south axis). The azimuth takes positive values $[+180°, 0°[$ when the sun is eastward, negative values $]0°, -180°]$ when it is westward and it is zero when the sun is in the south. On the other hand, the zenith angle θ gives an indication for the sun altitude by measuring the angle between the orthogonal projection of the sun vector **s** to the xy-plane and the z-axis. The sun elevation θ_e angle is then given by $90° - \theta$.

An optimal SAT alignment would be lengthwise, parallel to the x-axis of the coordinate system, i.e. perpendicular to the east-west axis. If the environmental setting of the power plant prohibits an optimal alignment of the SAT superstructure, a deviation angle η occurs as illustrated in Fig. 2. As nomenclature we define $\eta < 0$ for a clockwise rotation and $\eta > 0$ for a counter-clockwise rotation. For simplicity, we do not rotate the SAT system, but the sun azimuth instead. The new sun azimuth becomes

$$\phi_\eta = \phi - \eta. \tag{1}$$

One can easily convert between polar and Cartesian coordinates using:

$$x_s = r \cos \phi_\eta \cdot \sin \theta_e \tag{2}$$
$$y_s = r \sin \phi_\eta \cdot \sin \theta_e \tag{3}$$
$$z_s = r \cos \theta_e. \tag{4}$$

2.1. Sun path mirroring

The sun starts its course early in the east, reaches the south around noon and ends its path in the evening in the west. The course of the sun is always symmetric with regards to the north-south axis. This fact is exploited to further simplify the subsequent calculations: A variable δ is introduced, according to:

$$\delta = \begin{cases} +1, & \text{sun is in the east: } \phi_\eta \in]0, 180] \\ -1, & \text{sun is in the west: } \phi_\eta \in [-180, 0[\end{cases}$$

Using δ, the system behaviour must only be calculated once during simulation for either west or east. The results are then mirrored to get the final result.

2.2. Plane inclination

Solar power plants are sometimes installed on non-plane surfaces - for example in hilly environment. The inclination of the surface must be taken into account for precise tracking. The scheme for a non-plane setting is illustrated in Fig. 3. To keep all calculations as simple as possible, the plane inclination is embedded into the SAT rotation angle by following the update rule:

$$\alpha = \alpha - \delta \cdot \beta. \tag{5}$$

3. Basic tracking

According to Lambert's law, the yield of a solar module is directly proportional to angle of incidence γ between the sun light and the module normal vector for a given insolation intensity. The lower the angle, the higher the irradiation intensity, the higher the yield. Since the loss in irradiation intensity follows the function $cos\gamma$, maximal yield can only be achieved when the sun vector is orthogonal to the module plane, i.e. $\gamma = 0$. A single axis tracker can not always achieve orthogonality (as opposed to a DAT) due to the mechanical restrictions that apply, but the yield can be optimized during the span of one day. This section aims to

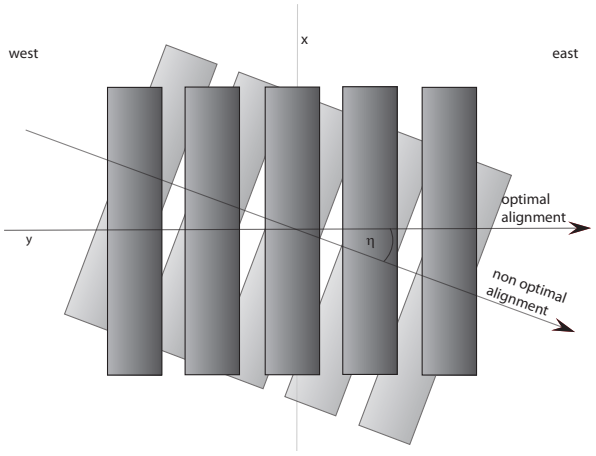

Fig. 2: Explanatory scheme for the SAT miss-alignment angle η. The system is not optimally aligned on the east-west axis (y-axis) for $\eta \neq 0$.

express the system rotation angle α as a function of the sun position on order to achieve maximum yield.

Let the module plane of one SAT be denoted as **P**, cf. Fig. 1.b. **P** can be rotated around the x-axis with the rotation angle α but has no other degrees of freedom. This way, **P** can be expressed in matrix notation:

$$\mathbf{P} = \begin{bmatrix} 1 & 0 \\ 0 & \cos\alpha \\ 0 & \sin\alpha \end{bmatrix} \tag{6}$$

The angle α is negative when **P** is inclined eastward, positive when **P** is inclined westward. The origin of co-ordinates $\mathbf{O} = [0,0,0]^T$ is placed as indicated in Fig. 4. A normal vector **v** of **P** can be expressed by:

$$\mathbf{v} = det\ \mathbf{P} = \begin{vmatrix} 1 & 0 \\ 0 & \cos\alpha \\ 0 & \sin\alpha \end{vmatrix} = \begin{bmatrix} 0 \\ -\sin\alpha \\ \cos\alpha \end{bmatrix} \tag{7}$$

As mentioned earlier, maximal yield is equivalent to a minimal angle γ between the normal vector **v** and the sun vector **s**. This can be achieved by minimizing the absolute value of the cross product **n** between the two vectors:

$$\mathbf{n} = \mathbf{v} \times \mathbf{s} = \begin{bmatrix} 0 \\ -\sin\alpha \\ \cos\alpha \end{bmatrix} \times \begin{bmatrix} x \\ y \\ z \end{bmatrix} = \begin{bmatrix} y\cos\alpha + z\sin\alpha \\ x\cos\alpha \\ x\sin\alpha \end{bmatrix} \tag{8}$$

Minimizing the absolute value of (8) corresponds to minimize the area of the parallelogram that the two vectors span and hence to minimize the angle between them:

$$\begin{aligned} |\mathbf{n}| &= \sqrt{(y\cos\alpha + z\sin\alpha)^2 + (x\cos\alpha)^2 + (-x\sin\alpha)^2} \\ |\mathbf{n}|^2 &= (y\cos\alpha + z\sin\alpha)^2 + (x\cos\alpha)^2 + (x\sin\alpha)^2 \\ &= (y\cos\alpha + z\sin\alpha)^2 + x^2 \end{aligned} \tag{9}$$

From (9) it can be seen that perfect SAT alignment (i.e $|\mathbf{n}|^2 = 0$) can only be achieved when the sun is positioned

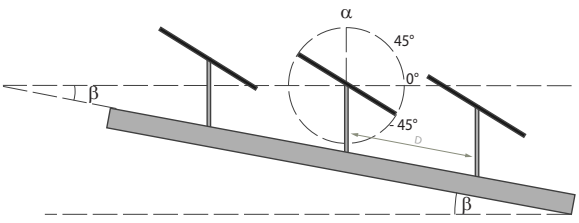

Fig. 3: Illustration of the plane inclination angle β for hilly environements.

on the east-west axis ($x^2 = 0$). The best SAT rotation angle for a given sun position can be found when

$$0 = y\cos\alpha + z\sin\alpha \tag{10}$$

applies. Solving for α and applying (5) gives

$$\alpha = \arctan\left(-\frac{y}{z}\right) - \delta \cdot \beta \tag{11}$$

as optimal rotation angle. Care needs to be taken when the sun rises or sets, i.e. $z = 0$.

4. Backtracking

Equation (11) allows the system to find an optimal rotation angle for a given sun position at any time. However, the case is not considered when for specific sun positions, self-shading may occur between adjacent SATs. The problem is illustrated for a two unit SAT in Fig. 4. With more units, the problem becomes even more important. In order to maximize the yield, shading should be avoided by all means, even though a shadow free position is not optimal in terms of the module-sun alignment as discussed in section 3. Smart control algorithms should be able to detect when SAT self-shading occurs and hence update the current rotation angle so that no shading can occur, while still optimizing the module alignment for maximum yield. This procedure is known as *backtracking*. The following section derives the equations for a shadow free SAT backtracking control mechanism that maximizes the electrical yield.

To begin with, it must be checked if self-shading occurs for a given sun vector **s**. As illustrated in Fig. 4, the module surface of two adjacent SATs with width A and height H will be denoted as F_1 and F_2, respectively. The origin of co-coordinates is placed in the center of gravity of F_1. In order to calculate if a shadow is cast from F_1 to F_2, one may project the corner point **p** of the surface F_1 onto the surface F_2 along the sun vector **s**. The point **p** can be expressed in Cartesian coordinates as:

$$\begin{aligned} \mathbf{p} &= \begin{bmatrix} \frac{A}{2} & y_p & z_p \end{bmatrix}^T, \text{ with} \\ y_p &= \frac{D}{2}\cos\alpha \\ z_p &= \frac{D}{2}\sin\alpha \end{aligned}$$

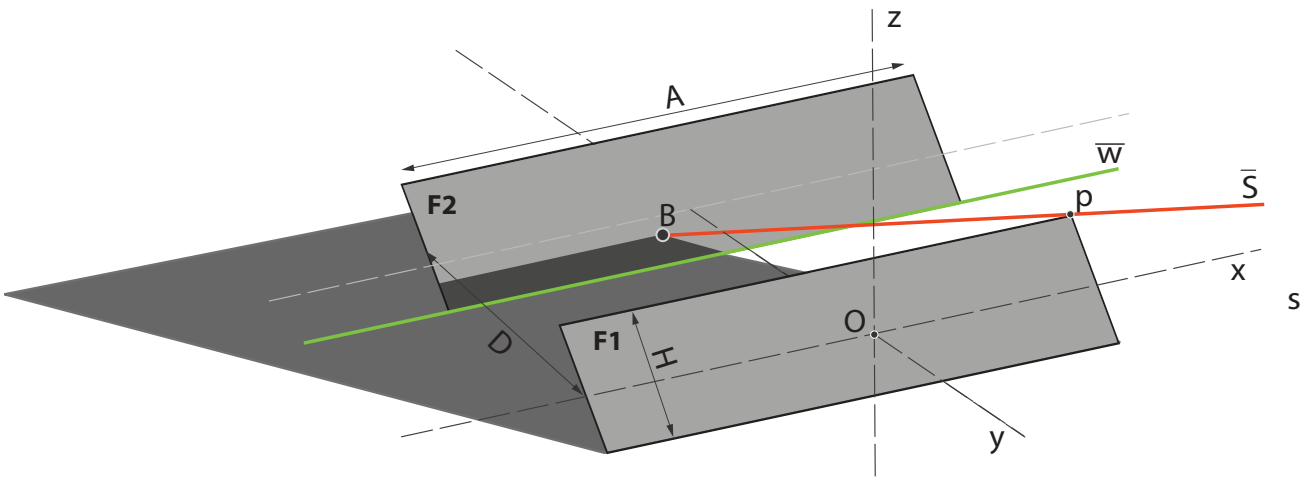

Fig. 4: Illustration of planes, lines and points needed for the derivation of the backtracking algorithm: A shadow is cast from surface $F1$ to surface F_2. By rotating the SAT so that line $\bar{\mathbf{s}}$ and line $\overline{\mathbf{w}}$ intersect, shading can be avoided by guaranteeing a minimal derivation from the optimal rotation angle.

The line $\bar{\mathbf{s}}$ that passes through $\mathbf{p}$ and is parallel to the sun vector $\mathbf{s}$ can be expressed as:

$$\bar{\mathbf{s}} : \mathbf{p} + \lambda \mathbf{s}. \tag{12}$$

According to equation (7), the normal vector $\mathbf{v}$ of the surface F_1 corresponds to:

$$\mathbf{v} = \begin{bmatrix} 0 \\ -\sin\alpha \\ \cos\alpha \end{bmatrix} \tag{13}$$

The plane that the surface F_2 is part of can be parametrized by

$$F_{2,plane} : \mathbf{v} \cdot \mathbf{r} - b = 0, \tag{14}$$

where $\mathbf{r}$ is an arbitrary point on the plane and b is a constant that must be determined. We choose $\mathbf{r} = \begin{bmatrix} 0 & D & 0 \end{bmatrix}^T$ and rearrange for b to find

$$b = -D \sin\alpha. \tag{15}$$

Insertion of (12) for the vector $\mathbf{r}$ into (14) and rearranging for λ gives:

$$\begin{aligned} &\mathbf{v} \cdot (\mathbf{p} + \lambda \mathbf{s}) - b = 0 \\ &\Rightarrow \lambda = \frac{b - \mathbf{v} \cdot \mathbf{p}}{\mathbf{v} \cdot \mathbf{s}} = \frac{b}{\mathbf{v} \cdot \mathbf{s}} \\ &= -\frac{D \sin\alpha}{z_s \cos\alpha - y_s \sin\alpha} \end{aligned} \tag{16}$$

We are now in the position to detect if shading from surface F_1 onto F_2 occurs: By inserting (16) into (12), one finds the Cartesian coordinates of the plane-line intersection point $\mathbf{B}$ (cf. Fig. 4). Since $\mathbf{B}$ can lie anywhere on the plane and must not necessarily lie on the surface F_2, an interval-check must be done to test if $\mathbf{B}$ is inside the bounding-box of F_2. If the check is positive, shading occurs and a new, shadow free rotation angle should be found.

If shading occurs, the tracker should be rotated as far as the lower bound of the surface F_2 (green line in Fig. 4 denoted as $\overline{\mathbf{w}}$) intersects with the line $\bar{\mathbf{s}}$. The line $\overline{\mathbf{w}}$ can be parametrized by

$$\overline{\mathbf{w}} : \begin{bmatrix} -\frac{A}{2} + \mu \cdot A \\ -y_p + D \\ -z_p \end{bmatrix} \tag{17}$$

To find the rotation angle that avoids shading, the intersection point between $\mathbf{s}$ and $\mathbf{w}$ must be found by equalizing the line expressions:

$$\begin{aligned} &\overline{\mathbf{w}} = \bar{\mathbf{s}} \\ &\Rightarrow \begin{bmatrix} -\frac{A}{2} + \mu \cdot A \\ -\frac{D}{2}\cos\alpha + D \\ -\frac{D}{2}\sin\alpha \end{bmatrix} = \begin{bmatrix} \frac{A}{2} + \lambda \cdot x_s \\ \frac{D}{2}\cos\alpha + \lambda \cdot y_s \\ \frac{D}{2}\sin\alpha + \lambda \cdot z_s \end{bmatrix} \end{aligned} \tag{18}$$

This gives us a nonlinear system with three unknowns (α, λ, μ) and three equations that we solve numerically to find two solutions for the shadow free rotation angle (including (5)) α_{sf}:

$$\alpha_{sf,1} = \arccos\frac{a - \sqrt{b}}{c} - \delta \cdot \beta \tag{19}$$

$$\alpha_{sf,2} = \arccos\frac{a + \sqrt{b}}{c} - \delta \cdot \beta \tag{20}$$

where

$$\begin{aligned} a &= H \cdot D \cdot z_s^2 \\ b &= H^4 y_s^4 + H^4 y_s^2 z_s^2 - H^2 D^2 y_s^2 z_s^2 \\ c &= H^2 y_s^2 + H^2 z_s^2 \end{aligned}$$

The actual values for λ and μ are of no interest for our problem. It is intuitive that the system angle α_{sf} should be minimal. Obviously equation (19) doesn't meet this requirement what leaves us with the final solution (20) for the best, shadow free backtracking angle.

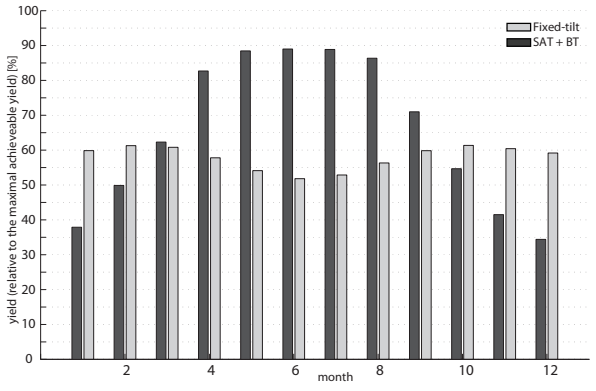

Fig. 5: Comparison of fixed-tilt yields and SAT yields for each month of a year. The results are relative to normed to the maximum yield that could be achieved with perfectly aligned module plane.

The proposed backtracking algorithm has been tested in the desert of Arizona with a real SAT system. The algorithmic framework proved to be exact at centimetre precision. Meanwhile, more than 100MW of SATs worldwide are controlled using the proposed scheme.

5. Results

Equations (20) and (11) allow to find an optimal, shadow free operation angle for the SAT. However, the exact position of the sun is needed for a given time and location. For that purpose, this paper uses the sun position algorithm proposed in [9], that allows to determine the sun azimuth and elevation with an accuracy of $\pm 0.0003^\circ$ without the need of any additional sensors or hardware. In fact, the sun position algorithm can run on the same controller as the tracking control which is beneficial in terms of costs and installation complexity. Fig. 6 shows a simulation of the SAT behaviour during one day in January for the location Berlin, Germany. The shadow free angle of operation α_{sf} and the optimal angle α are plotted against the time. Additionally, the sun azimuth and elevation are shown. The angle α_{sf} is limited to a range of $[-45, 45]$ degrees, which is due to mechanical limitations that apply to a real-world constructions. As a matter of fact, all SATs are provided with a rotation limit which may vary between 45° and 60°, depending on the design. The system switches to backtracking as soon as the sun rises and continues shadow free tracking until about 10 am. Afterwards, no shading occurs any more and the system's angle of operation corresponds to the optimal angle until about 2.30 pm when the sun elevation declined enough to cause shading again.

The results were further used to simulate the relative extra yield of a SAT compared to an optimally aligned fixed-tilt superstructure at the same location, cf. Fig. 5. The shown results are normed to the maximal achievable yield. It can be seen, that the SAT clearly outperforms the fixed-tilt installation in the summer months, when the sun stands high in the sky and the days are long. In the winter months the fixed-tilt installation performs better because the sun stands low in the sky, shadows are more likely and the SAT system often switches to backtracking and hence misses the optimal alignment to the sun. However, the results are relative to the maximal achievable yield and have no information about the absolute annual extra yield. Fig. 7 shows the simulation results for the total, absolute extra yield of a SAT compared to an optimally aligned fixed-tilt installation. The plot shows the extra yield plotted against the latitude. The clear-sky insolation model proposed in [10] has been used for this purpose. It is interesting to see how minimal gain can be achieved for latitudes of around 50° to 60°, which corresponds to central Europe. Here, the simulation predicts an extra yield of about 8-10%, which is consistent with the results found by other researchers [11]. According to Fig. 7, the usage of a SAT system becomes very lucrative for southern countries, where the gain may rise up to 30%.

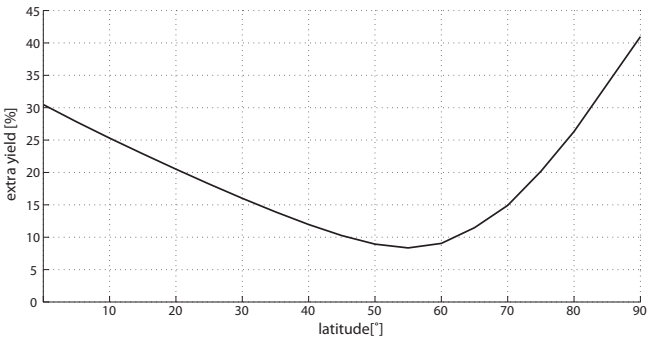

Fig. 7: Averaged, annual extra yield of a SAT compared to an optimally aligned fixed-tilt superstructure in dependence on the latitude.

Finally, the effect of the spacing D between two adjacent SATs has been investigated in this work. Fig. 8 summarized the results. It can be seen that in general the best distance in terms of extra gain and space efficiency can be achieved for a distance of about 12 meters when the slope of the curve flattens out. However the best distance strongly depends on the park layout and generally needs to be selected individually for every park.

When dealt with diffuse insolation (which forms a major part of central Europe's insolation) a totally flat tracker would be the best operational position. Theoretically, the maximum amount of light could be collected in this position. However, to detect the current type of insolation, extra sensors are required. Alternative solutions could employ local weather broadcasts to adapt the tracking behaviour in order to avoid external hardware.

6. Conclusions

We proposed an algorithmic framework to control photovoltaic single-axis-trackers using backtracking. The control schemes are able to maximize the electrical yield of a

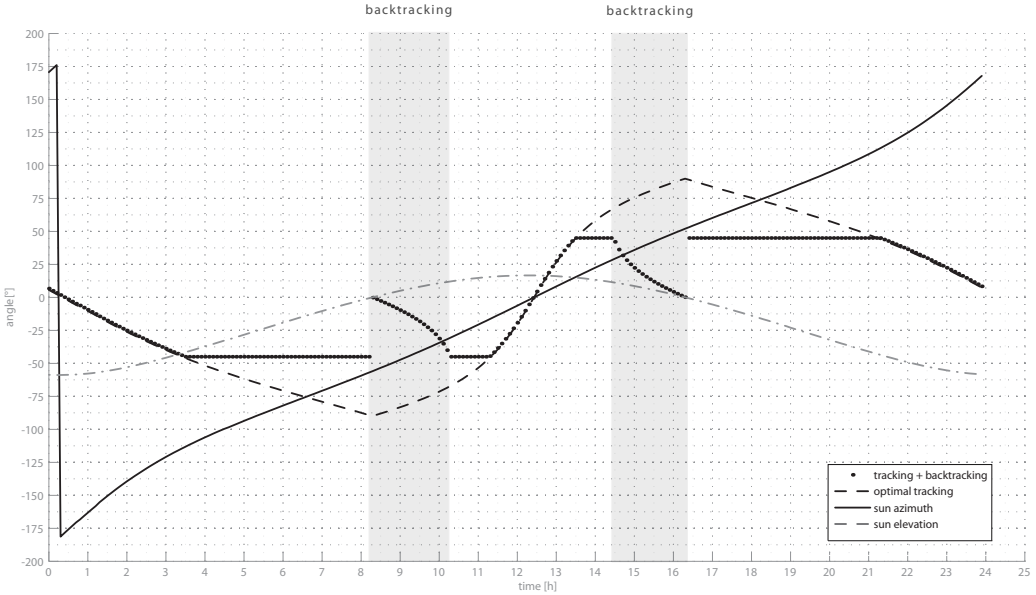

Fig. 6: Tracking and backtracking angles, sun azimuth and elevation plotted for the 1st of January 2012 in Berlin. The maximal rotation angle has been clipped to $\pm 45°$. As the sun elevation angle is low, backtracking occurs from 8 am to 10 am such as 14.30pm and 16.30pm.

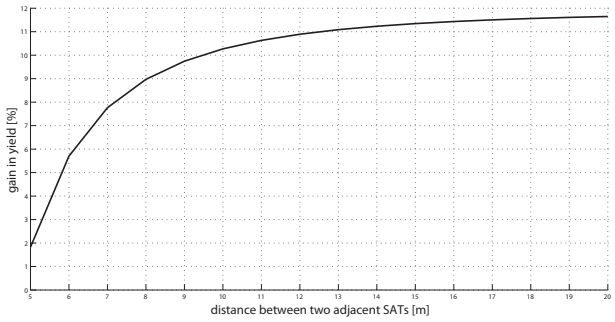

Fig. 8: Averaged, annual extra yield of a SAT compared to an optimally aligned fixed-tilt superstructure in dependence of the distance D between two adjacent SAT units.

SAT power-plant by finding the best, shadow free rotation angle for the tracker in dependence of its location and environmental settings. By simulating, SAT yields have been compared to fixed-tilt yields giving insight into the system strengths and weaknesses. The proposed controlling scheme is field tested and is used in power plants with more than 100MW output world wide.

References

[1] KATHIBÁ, T.N, MOHAMED, A., KHAN, R.J, AMIN,N., A Novel Sun Tracking Controller For Photovoltaic Panels, In *Journal of Applied Sciences 9* (22):4050-4055,2009

[2] CATARIUS, A., CHRISTINER, M., Azimuth-Altitude Dual Axis Solar Tracker *Bachelor Thesis*, Worcester Polytechnic Institute, 2010

[3] PETERSON, T., RICE, J., VALENTINE, J., Solar Tracker, *Final Project Report*, Cornell University, 2005

[4] LORENZO, E., NAVARTE, L., MUOZ, J., Tracking and Back-Tracking, In *Progress in Photovoltaics: Research and Applications* (19): 747-753; DOI: 10.1002/pip.1085, 2011

[5] LORENZO, E., PEREZ, M., EZPELETA, A., ACEDO, J., Design of Tracking Photovoltaic Systems with a Single Vertical Axis, In *Progress in Photovoltaics: Research and Applications* (10): 533-543; DOI: 10.1002/pip.442, 2002

[6] SEME, S., STUMBERGER, G., VORSIC, J., Maximum Efficiency Trajectories of a Two-Axis Sun Tracking System Determined Considering Tracking System Consumption, In *IEEE Transactions on Power Electronics* (26): 1280-1290, 2011

[7] PAVLOVIC, T.M., MILOSAVLJEVIC, D.D., RADIVOJEVIC, A.R., PAVLOVIC, M.A., A Comparison And Assesment Of Electricity Generation Capacity for Different Types of Photovoltaic Solar Plants of 1 MW in Sokobanja, Serbia, In *Thermal Science* (15): 605-618, 2011

[8] KING, D.L., BOYSON, W.E.., KRATOCHVIL, J.A., Analysis of Factors Influencing the Annual Energy Production of Photovoltaic Systems, In *Photovoltaic Specialists Conference*; DOI: 1356-1361;10.1109/PVSC.2002.1190861, 2003

[9] REDA, I., ANDREAS, A., Solar Position Algorithm for Solar Radiation Applications, In *Solar Energy 7*(5): 577-589, 2004

[10] KELLER, B., COSTA, A.M.S., A Matlab GUI for calculating the solar radiation and shading of surfaces on the earth, In *Computer Applications in Engineering Education 19*(1): 161-170, 2009

[11] VANICEK, P., STEIN, S., Simulation of the Impact of diffuse Shading On the Yields of Large Single Axis Tracked PV-Plants, In *Technical Report*,Deutsche Gesellschaft fuer Sonnenenergie LV Berlin Brandenburg e.V., 2009

About Authors...

DORIAN SCHNEIDER was born in Berlin, Germany. He received his diploma degree in electrical engineering in 2009 from the Technical University of Berlin and his masters degree in signal processing from the Jiao Tong University Shanghai in 2008. After graduating, he worked as a system engineer for a german solar company. In 2010 he joined the institute of imaging and computer vision at the RWTH University Aachen to follow up is Ph.D. in the field of pattern analysis and computer vision.